

# The influence of the acid sites on the methylamines synthesis with Cu-HZSM-5 zeolite

Maria Helena de Oliveira Nunes<sup>a</sup>, Victor Teixeira da Silva<sup>b</sup>, and Martin Schmal<sup>a,\*</sup>

<sup>a</sup>NUCAT/PEQ/COPPE/Federal University of Rio de Janeiro (UFRJ), Cidade Universitária, Bloco G, sala 128, Ilha do Fundão, Rio de Janeiro/RJ, Brasil, CEP: 21945-970

<sup>b</sup>Instituto Militar de Engenharia, Departamento de Engenharia Química, Praça General Tibúrcio, 80, Praia Vermelha, Rio de Janeiro/RJ, Brasil, CEP: 22290-270

Received 30 January 2004; accepted 11 May 2004

There is a high industrial demand for MMA and DMA, however, the production of TMA is favored with the commercial catalysts. This work tested the methanol amination reaction with HZSM-5 and Cu/HZSM-5 zeolites (%Cu = 1.2, 3.7 and 6.0). Regarding the MMA selectivity, light differences were observed among Cu/HZSM-5 catalysts and pure zeolite, although the catalysts containing 3.7% copper was slightly more selective to MMA than the other metallic catalysts studied. From these results it is suggested that the metal loading present in the catalysts leads to a modification in the nature of the acidic sites, in particular, the selectivity depends on ratio Brønsted/Lewis acid sites. This modifications would facilitate the amines desorption during the reaction.

**KEY WORDS:** acid sites; methylamines synthesis; Cu-HZSM-5 zeolite.

## 1. Introduction

Methanol conversion in valuable products makes it an important raw material to the wide miscellaneous chemicals. Acetic acid, propionic acid, acetic anhydride, ethylene glycol, ethanol and amines are good examples of products that have already been successfully synthesized using methanol as feedstock [1]. Among the materials that can be obtained from methanol, the low molecular weight aliphatic amines occupy an important place in modern society because of their large application possibilities. Mono-, di- and tri-methylamines (MMA, DMA and TMA) are normally used as corrosion inhibitors, probe molecules to characterize superficial acidity of solid materials, softeners for synthetic fibers, scatters to paints and pigments and like intermediates in chemical and pharmaceutical industries (production of pharmaceutical product, pesticides, explosives and animals feed).

Methylamines are synthesized industrially, using methanol and ammonia and acid catalysts (e.g. alumina or silica–alumina) that approaches the thermodynamic equilibrium molar ratio MMA : DMA : TMA (17 : 21 : 62 at  $T = 673$  K and molar ratio  $\text{NH}_3/\text{CH}_3\text{OH} = 1$ ). Close to the thermodynamic equilibrium the TMA production is favored, and therefore the demanding products MMA and the DMA become more important [2]. For increasing production of MMA and DMA it is necessary to recycle TMA, but it makes the process more expensive. To

minimize costs involved for separation of TMA and to increase the production of MMA and DMA, recent research have developed zeolite catalysts [3,4]. According to literature, the product distribution and the enhancement of MMA selectivity are related to pore sizes of zeolites in this reaction (shape selectivity). It can be explained either by the retention of TMA in the pores or by the reaction of these molecules inside the pores.

The literature did not present new catalysts able to increase the MMA and DMA selectivity to reach the molar ratio 33 : 53 : 14 (MMA : DMA : TMA) required in industrial processes. There are continuously publications in this area [5]. An interesting observation is that there are only few reports concerning the employment of transition metals modified zeolites for this kind of reaction, although copper catalysts on different supports, such as  $\text{Al}_2\text{O}_3$ ,  $\text{Cr}_2\text{O}_3$  and  $\text{Cr}_2\text{O}_3\text{--SiO}_2$ , are highly efficient for the catalytic amination of alcohols [6].

The main goal of this paper is to test the Cu/HZSM-5 catalysts and how it affects the molar relation of amines produced in methanol amination reaction. Besides, different characterization techniques were employed to determine the effect of the metal and acidic properties on the selectivity and activity.

## 2. Experimental

### 2.1. Catalysts preparation

HZSM-5 zeolite from DEGUSSA (SAR = 28.4) was previously calcined at 803 K for 4 h ( $5 \text{ K min}^{-1}$ ) in a pyrex glass calcinator under continuous air flow

\*To whom correspondence should be addressed.  
E-mail: schmal@peq.coppe.ufrj.br

(30 mL min<sup>-1</sup>) before the preparation. This prior treatment was necessary to stabilize the zeolite structure and to eliminate undesirable materials, like as residual templates.

The catalysts were prepared using three different methodologies of preparation:

- (1) Ionic exchange
- (2) Step 1: Ionic exchange  
Step 2: Precipitation (pH = 7.0 with NH<sub>4</sub>OH)
- (3) Step 1: Ionic exchange  
Step 2: Precipitation (pH = 9.0 with NH<sub>4</sub>OH and pH = 7.0 with HNO<sub>3</sub>)

The ionic exchange step consisted by adding a known amount of HZSM-5 zeolite (SAR = 28.4) to a copper nitrate solution (0.90 N) and maintaining the mixture under agitation during 20 h at 353 K. Methods (2) and (3) were applied after ionic exchange and submitted to a second step, the precipitation (step 2). This later one consisted by adjusting the pH solution to the desired value (7.0 or 9.0) with NH<sub>4</sub>OH, according the procedure defined by Iwamoto *et al.* [7]. Then the samples were filtered, washed, dried at 373 K (16 h) and calcined (under air flow) for 6 h up to 773 K (30 mL min<sup>-1</sup>). Another catalyst was prepared adjusting the pH to 9.0 with NH<sub>4</sub>OH and then to 7.0 with HNO<sub>3</sub>.

## 2.2. Temperature programmed reduction (TPR)

TPR measurements were performed as described elsewhere [8], with a thermal conductivity detector (TCD) and an acquisition program (PeakSimple II/Chromatography Software). Prior the analysis the samples were dried from 298 to 503 K under Ar flow (10 K min<sup>-1</sup> and 30 mL min<sup>-1</sup>) for 30 min and then cooled to room temperature. After this step the Ar flow was switched to a mixture 1.6% H<sub>2</sub>/Ar (30 mL min<sup>-1</sup>) raising the oven temperature from 298 to 803 K at 5 K min<sup>-1</sup>.

## 2.3. Temperature programmed reaction (TPSR)

### 2.3.1. Temperature programmed reaction of NH<sub>3</sub> prior adsorbed and CH<sub>3</sub>OH/He flow

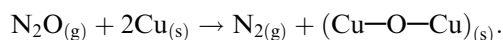
Initially the catalyst was reduced by flowing H<sub>2</sub> (30 mL min<sup>-1</sup>) and rising the temperature from 298 to 803 K (5 K min<sup>-1</sup>), held constant for 30 min at this temperature and cooled down to room temperature. Then a mixture 4% NH<sub>3</sub>/He was admitted to the reactor (50 mL min<sup>-1</sup>) and maintained for about 1 h. The reactant was outflowed with He (50 mL min<sup>-1</sup>) until total removal of the residual NH<sub>3</sub>. Then, the flow was switched to a mixture 21% CH<sub>3</sub>OH/He (50 mL min<sup>-1</sup>) and the temperature raised continuously at 10 K min<sup>-1</sup> up to 803 K. The reactor downstream was followed by a quadrupole mass spectrometer.

### 2.3.2. Temperature programmed reaction of CH<sub>3</sub>OH prior adsorbed and NH<sub>3</sub>/He flow

Similarly, the catalysts were reduced as described above. Then a mixture 21% CH<sub>3</sub>OH/He was admitted to the reactor (50 mL min<sup>-1</sup>) and maintained for about 1 h. The reactant was totally outflowed with a He flow (50 mL min<sup>-1</sup>) prior switching to a mixture 4% NH<sub>3</sub>/He (50 mL min<sup>-1</sup>) flow and the temperature raised continuously at 10 K min<sup>-1</sup> up to 803 K. The reactor downstream was analyzed by a quadrupole mass spectrometer.

## 2.4. Oxidation with N<sub>2</sub>O (determination metallic surface area)

The methodology for the determination of the metallic surface area was performed according to Bond and Namijo [9]. The first step consisted by reducing the metal as described above in the TPR and then cooling down to 363 K. Then the flowing gas was switched to a mixture 10% N<sub>2</sub>O/He (80 mL min<sup>-1</sup>) where the sample was submitted to an oxidant atmosphere for 20 h (1,2 and 3,7 CuZ) and 24 h (6,0 CuZ). After superficial oxidation the sample was cooled to room temperature under Ar flow and switched to the reduction mixture. This technique is basically the decomposition of N<sub>2</sub>O molecules on copper surface according to the reaction



The H<sub>2</sub> consumption in the second reduction cycle (Cu<sub>2</sub>O + H<sub>2</sub> → 2Cu + H<sub>2</sub>O) allows us to calculate the surface copper area, according following equation [8]

$$S_M = \frac{2 \times n_{\text{H}_2} \times 6.02 \times 10^{23} (\text{at/gmol})}{1.4 \times 10^{19} (\text{at/m}^2) \times m_{\text{cat}} (\text{g})},$$

where  $S_M$  – Metallic area, m<sup>2</sup>/g<sub>cat</sub>,  $n_{\text{H}_2}$  – H<sub>2</sub> consumption in the second TPR cycle, gmols,  $m_{\text{cat}}$  – Catalyst weight, g.

## 2.5. Infrared of pyridine adsorption (FTIR-Py)

By adsorbing pyridine followed by infrared measurements it was possible to verify the influence of the methodology used in preparation method and the formation and nature of acid sites present in the catalyst. The analysis was performed in a PERKIN-ELMER apparatus (model SYSTEM 2000 FTIR) and the samples were analyzed on a self-made pastille. The IR spectrum registered bands between 450 and 4000 cm<sup>-1</sup>.

The acid sites concentration was calculated for each catalyst using the Lambert–Beer equation:  $A = \varepsilon \times L \times C$  where

$A$  – absorbance in a determined wave length, a.u. Brönsted (1540 cm<sup>-1</sup>), Lewis (1450 cm<sup>-1</sup>),  $\varepsilon$  – molar extinction coefficient: Brönsted (0.059 ± 0.004) cm<sup>2</sup>/μmol, Lewis (0.084 ± 0.003) cm<sup>2</sup>/μmol.  $L$  – pastille

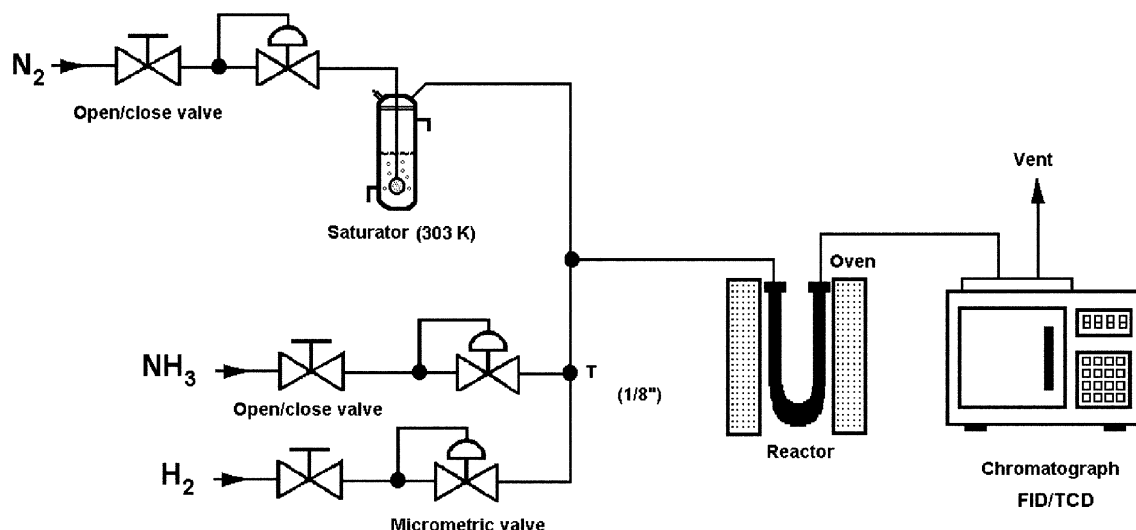


Figure 1. Experimental apparatus scheme.

thickness (or optical way traveled through the incident light).

Prior to the analysis the samples were dried from 298 to 503 K under inert Ar flow ( $10 \text{ K min}^{-1}$  and  $30 \text{ mL min}^{-1}$ ) for 30 min and then cooled to room temperature. After evacuation the sample was cooled to 273 K and pyridine was admitted into the reactor for 1 h. Then, after a second evacuation the temperature was raised continuously up to 298 K and the IR spectrum registered. The analysis was performed using the spectrum of dried samples as background.

## 2.6. Catalytic tests

The samples were catalytically evaluated in a continuous micro reactor flow specially built for this purpose at atmospheric pressure (figure 1).

Methanol was fed to the reactor through the saturator, kept at 303 K and flowing  $\text{N}_2$  as carrier gas. The  $\text{CH}_3\text{OH}$  flow was maintained at  $85 \text{ mL min}^{-1}$  ( $\text{NH}_3/\text{CH}_3\text{OH} = 1$ ) and the mass of catalyst was 0.4 g. The reaction was studied for five different temperatures (573, 623, 673, 723 and 773 K). Products and the reactants were analyzed by gas chromatography (GC).

Before reaction the catalysts were reduced under flowing  $\text{H}_2$ , as described above for TPR, and cooled down to the reaction temperature. The products were quantified considering total amines, calibrated previously from reliable pattern solutions. The selectivity values for each amine was calculated using the equation below and compared to the molar ratio 33 : 53 : 14 (MMA : DMA : TMA) required for the industrial processes and used as parameter for the selection of a suitable catalyst for this reaction.

$$S_{\text{MMA}} = \frac{Y_{\text{MMA}}}{Y_{\text{MMA}} + Y_{\text{DMA}} + Y_{\text{TMA}}},$$

where  $F_{\text{MeOH}}$  – methanol molar flow,  $\text{mols}_{\text{MeOH}} \text{ min}^{-1}$ ,  $Y_{\text{MMA}}$  – MMA molar ratio in the reactor downstream,  $Y_{\text{DMA}}$  – DMA molar ratio in the reactor downstream,  $Y_{\text{TMA}}$  – TMA molar ratio in the reactor downstream.

## 3. Results and discussion

### 3.1. The reduction degree and metallic area

The metal content of the different copper catalysts are presented in table 1. The addition of  $\text{NH}_4\text{OH}$  to the solution after the ion exchange step provided a significant increase of copper amount, as shown in table 1. The possible explanation of this result is the formation of  $\text{Cu}(\text{OH})^+$  and  $\text{Cu}(\text{OH})_2$  in neutral pH [10]. After calcination these species are transformed into CuO particles at the external surface of the zeolite. The Cu/HZSM-5 catalyst prepared by wet impregnation [11] presented after calcinations a blue color and small black granules, which are associated to bulk, agglomerated CuO with low interaction with the zeolite at the external surface. On the other hand, when the catalyst was prepared controlling the pH value after ionic exchange, Cu was homogeneously distributed. Interesting is that the Cu content in the sample prepared with successive

Table 1  
Chemical analysis of the Cu/ZSM-5 catalysts<sup>a</sup>

| Preparation Method             | % Cu (p/p) | Designation |
|--------------------------------|------------|-------------|
| Ionic exchange                 | 1.2        | 1,2 CuZ     |
| Ionic exchange                 |            |             |
| Precipitation (pH 7.0)         | 3.7        | 3,7 CuZ     |
| Precipitation (pH 9.0)         | 3.8        | 3,8 CuZ     |
| Precipitation (pH 9.0 and 7.0) | 6.0        | 6,0 CuZ     |

<sup>a</sup>The metallic values were obtained by Atomic Absorption.

pH adjustment after ionic exchange (6,0 CuZ) increased 62% when compared to the samples prepared at a fixed pH (3,7 CuZ). This behavior is probably related to the  $\text{HNO}_3$  addition during the preparation, because during the pH adjusting, using  $\text{NH}_4\text{OH}$ , part of the copper present in the solution exists as ammoniac complex. It is destroyed during the addition of  $\text{HNO}_3$ , due to the formation of a more stable complex ( $\text{NH}_4^+$ ). During this process  $\text{Cu}^{2+}$  ions would be released in the solution and precipitate as  $\text{Cu}(\text{OH})_2$ .

The presence of two distinct copper species in Cu/HZSM-5 catalysts was also confirmed in the TPR results (figure 2).

According to the literature [12,13],  $\text{Cu}^{2+}$  species in the Cu/HZSM-5 catalysts can be reduced in successive steps with the formation of an intermediate oxidation state ( $\text{Cu}^{2+} \rightarrow \text{Cu}^{1+} \rightarrow \text{Cu}^0$ ). The literature reports that the reduction peaks are associated to following reactions:

- (A)  $(\text{Cu}-\text{O}-\text{Cu})^{2+} + \text{H}_2 \rightarrow 2\text{Cu}^0 + \text{H}_2\text{O}$
- (B)  $\text{Cu}^{2+} + 1/2 \text{H}_2 \rightarrow \text{Cu}^{1+} + \text{H}^+$
- (C)  $\text{CuO} + \text{H}_2 \rightarrow \text{Cu}^0 + \text{H}_2\text{O}$
- (D)  $\text{Cu}^{1+} + 1/2 \text{H}_2 \rightarrow \text{Cu}^0 + \text{H}^+$

The presence of oxocations  $[\text{Cu}-\text{O}-\text{Cu}]^{2+}$  was discarded, because in two successive reduction cycles at room temperature,  $\text{H}_2$  consumption was not observed. On the other hand, TPR analysis shows a large amount of  $\text{H}_2$  consumption in the first peak, compared to the second one for the catalysts with pH adjust after the ionic exchange step. It suggests the presence of two

copper species (probably  $\text{Cu}^{2+}$  and  $\text{CuO}$ ), which are reduced according to reactions (B) and (C), respectively. Therefore, peak 1 in samples 3,7 and 6,0 CuZ is the overlapping of peaks related to the reactions (B) and (C). It means,  $\text{Cu}^{1+}$  species would be reduced to  $\text{Cu}^0$  like reaction (D), which is represented by curve 2. Comparing the reduction peaks of sample 1,2 CuZ, the maximum temperature is higher than that of the other catalysts. The large peak demonstrates the presence of Cu species, which are more difficult to reduce, due to the strong interaction between Cu species and the zeolite framework.

Table 2 presents the  $\text{H}_2$  consumption and degree of reduction from TPR analysis. The degree of reduction was calculated considering the complete reduction of species  $\text{Cu}^{2+}$  ( $\text{Cu}^{2+} + \text{H}_2 \rightarrow \text{Cu}^0 + 2\text{H}^+$ ).

These results show complete reduction for  $\text{Cu}^{2+}$  and  $\text{CuO}$  for catalysts containing more than 3.7% of copper. For low Cu content the reduction degree is almost 83%. In consequence, the surface metallic area increased 10-fold by doubling the Cu content. It turns out that for 3.7% Cu in the zeolite the  $\text{Cu}^{2+}$  ions are reduced in sequence to  $\text{Cu}^{+1}$  and  $\text{Cu}^0$ , while for higher contents only  $\text{CuO}$  may reduce to  $\text{Cu}^0$ .

### 3.2. Activity and selectivity

The activity and selectivity results are shown in table 3. Preliminary tests indicate that the reaction rate can be determined considering a first order reaction.

$$(-r_A) = \frac{-\ln(1 - X_A)}{W_{\text{Cat}}/F_{\text{MeOH}}}$$

where  $(-r_A)$  = Reaction rate, moles<sub>MeOH</sub> g<sub>Cat</sub><sup>-1</sup> min<sup>-1</sup>,  $w_{\text{Cat}}$  = Catalysts weight, g.

Table 3 shows the reaction rate for different temperatures, as calculated from this equation. The reaction rate increases 2-fold with the introduction of Cu in the zeolite, but is not very sensitive for higher loading of Cu.

As shown in table 3, the distribution of amines (MMA:DMA:TMA) for different temperatures are still far from the required industrial processes. No significant differences for MMA were observed for pure zeolite and copper containing zeolites. However, comparing the selectivity of MMA at isoconversion, it turns out that the 3,7 CuZ samples was fairly more selective. The high selectivity for TMA at low temperatures is due to the

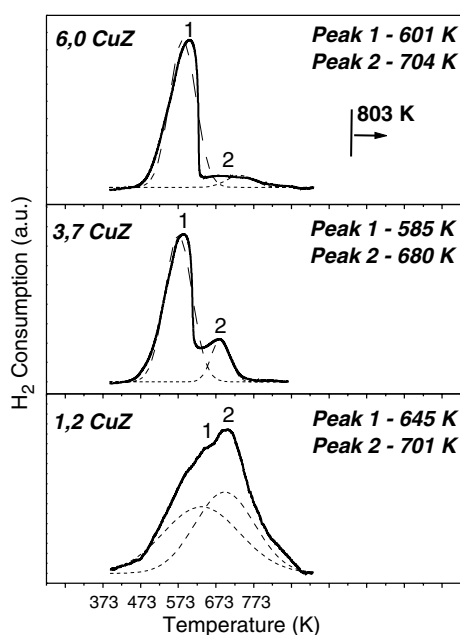


Figure 2. Cu/HZSM-5 catalysts TPR profiles. The dashed curves match to the peaks of deconvolution, considering two reduction peaks.

Table 2  
 $\text{H}_2$  consumption and degree of reduction results

| Sample  | $\text{H}_2$ consumption ( $\mu\text{mol/g}_{\text{Cu}}$ ) | Degree of reduction (%) | Metallic area $S_{\text{metallic}}$ ( $\text{m}^2/\text{g}_{\text{cat}}$ ) |
|---------|--|-------------------------|--|
| 1,2 CuZ | 12984 (155.8)  | 83                      | 1.95   |
| 3,7 CuZ | 15954 (480.4)  | 100                     | 20.8   |
| 6,0 CuZ | 16038 (782.2)  | 100                     | 31.8   |

Table 3  
Conversion and selectivity and reaction rates results

| Catalyst | $T_{\text{Reaction}}(\text{K})$ | $X_{\text{MeOH}}(\%)$ | $S_{\text{MMA}}(\%)$ | $S_{\text{DMA}}(\%)$ | $S_{\text{TMA}}(\%)$ | $(-r_A) \times 10^2$<br>(moles <sub>MeOH</sub> g <sub>Cat</sub> <sup>-1</sup> min <sup>-1</sup> ) |
|----------|---------------------------------|-----------------------|----------------------|----------------------|----------------------|---|
| HZSM-5   | 623                             | 14                    | 0                    | 0                    | 100                  | 14  |
|          | 673                             | 31                    | 0                    | 0                    | 100                  | 35  |
|          | 723                             | 46                    | 18                   | 12                   | 71                   | 59  |
|          | 773                             | 48                    | 18                   | 11                   | 70                   | 63  |
| 1,2 CuZ  | 673                             | 20                    | 0                    | 0                    | 100                  | 22  |
|          | 723                             | 79                    | 16                   | 10                   | 74                   | 150   |
|          | 773                             | 92                    | 19                   | 11                   | 71                   | 243   |
| 3,7 CuZ  | 573                             | 13                    | 0                    | 0                    | 0                    | 11  |
|          | 623                             | 54                    | 17                   | 10                   | 73                   | 59  |
|          | 673                             | 78                    | 21                   | 11                   | 68                   | 117   |
|          | 673                             | 80                    | 17                   | 13                   | 70                   |   |
|          | 723                             | 83                    | 25                   | 11                   | 65                   | 136   |
|          | 773                             | 87                    | 24                   | 10                   | 66                   | 156   |
| 6,0 CuZ  | 573                             | 6                     | 0                    | 0                    | 0                    | 6   |
|          | 623                             | 36                    | 0                    | 0                    | 100                  | 43  |
|          | 673                             | 74                    | 18                   | 10                   | 72                   | 128   |
|          | 673                             | 63                    | 18                   | 12                   | 70                   |   |
|          | 723                             | 89                    | 21                   | 11                   | 67                   | 210   |
|          | 773                             | 95                    | 23                   | 11                   | 66                   | 285   |

strong adsorption of MMA and DMA on the acid sites, favoring the transformation of those amines into TMA.

The literature has also reported deactivation of zeolites (coke formation) and zeolites containing copper (nitrite formation) during the methanol amination. Preliminary study was performed at 723 K and after 8 h and no deactivation was observed, contrasting the results of Mochida *et al.* [17]. Our results show similar values of selectivity for Cu catalysts and for pure HZSM-5, which is a strong indication of the absence of side reactions, such as amines desproportionation. In agreement with Jobson *et al.* [18] and Baiker and Kijenski [19] the amines desproportionation may affect strictly the desired product selectivity.

### 3.3. Influence of the acidity

Although the activity increased with the addition of Cu the selectivity was greatly affected and the main question arises how is the balance between the metallic and acidic sites affecting the selectivity. Therefore, infrared of pyridine adsorption was performed and results show quantitatively the formation of acid sites (Brönsted and Lewis sites) for catalysts HZSM-5 and Cu modified zeolites. The intensity bands 1540 and 1450 cm<sup>-1</sup> were taken and the concentrations were calculated (ratio between the Brönsted and Lewis acid sites concentration (*B/L* ratio) was calculated) with the corresponding molar extinction coefficients, as shown in table 4. The  $\Delta$  parameter is defined as the variation of  $A_{\text{Brönsted}}$  of CuZ catalysts in relation to pure zeolite

$$\Delta = \frac{A_{\text{Brönsted,HZSM-5}} - A_{\text{Brönsted,CuZ}}}{A_{\text{Brönsted,HZSM-5}}}$$

Table 4  
Brönsted/Lewis (B/L) ratio on Cu/HZSM-5 catalysts

| Catalyst | $A_{\text{Brönsted}}$ (u.a.) | $A_{\text{Lewis}}$ (u.a.) | B/L  | $\Delta$ (%) |
|----------|------------------------------|---------------------------|------|--------------|
| HZSM-5   | 0.7838                       | 0.2260                    | 4.94 | –            |
| 1,2 CuZ  | 0.4494                       | 0.2400                    | 2.67 | 42.66        |
| 3,7 CuZ  | 0.4712                       | 0.6406                    | 1.05 | 39.88        |
| 6,0 CuZ  | 0.3874                       | 0.9674                    | 0.57 | 50.57        |

$A_{\text{Lewis}}$  – absorbance related to the Lewis acid sites.

$A_{\text{Brönsted}}$  – absorbance related to the Brönsted acid sites.

Besides, the  $\Delta$  (%) values were used to estimate the degree of exchange of Cu in the Zeolite structure. For this zeolite, 100% corresponds to an exchange of 3.2% Cu. For 1,2 CuZ the exchange was 37.5%, which agrees very well with data presented in table 4. Notice that the catalyst 3,7 CuZ was approximately the same, which indicates the same degree of exchange.

The amounts of Lewis sites increases with Cu content while the Brönsted acid sites decrease, however, the total concentration of acid sites is approximately the same. As shown the Lewis acid sites increase with increasing Cu content, which indicates that the compensation of cations affected the Lewis acid sites.

Therefore, acid sites strength plays a fundamental role in the selectivity performance, however the nature of the acid sites may strongly influence the amines distribution. Figure 3 shows the selectivity as function of the Brönsted/Lewis ratio. For a ratio of approximately  $B/L = 1.0$  the selectivity to MMA is high, but at higher B/L ratio TMA prevails. It turns out that similar concentrations of B and L sites may influence acid

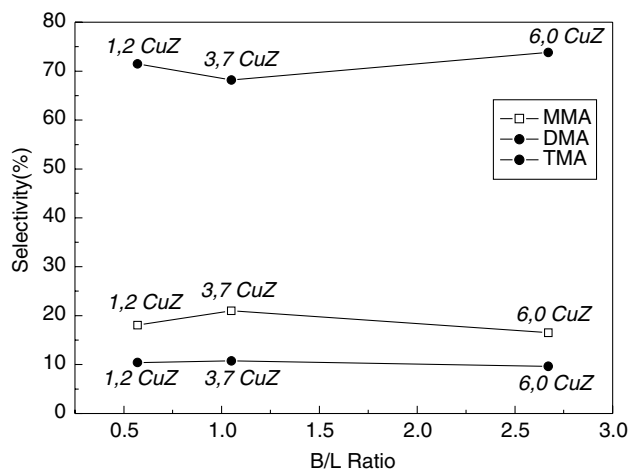


Figure 3. Selectivity as function of the ratio Brønsted/Lewis concentrations.

strengths, which in turn favors the reaction in terms of activity and selectivity to MMA.

Figure 4 presents the results of methanol conversion versus reaction temperature. As can be seen these catalysts show similar behavior regarding the methanol conversion up to approximately 673 K. However, the 3,7 CuZ and 6,0 CuZ catalysts were more active than HZSM-5 and 1,2 CuZ. Above 673 K the conversion of the 3,7 CuZ sample reach stabilization. The 1,2 CuZ sample presents a significant increase in the methanol conversion above 673 K.

For isoconversion around 20% (dashed line) the 3,7 and 6,0 CuZ catalysts are more active than HZSM-5

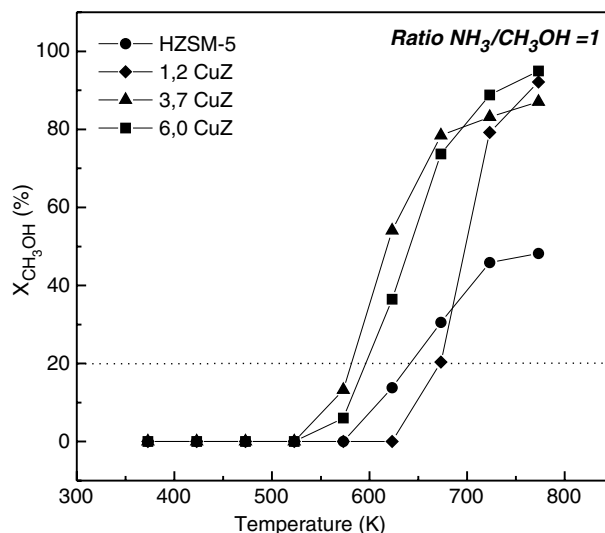


Figure 4. Methanol conversion versus reaction temperature.

zeolite. From these results the following activity pattern becomes

$$3,7 \text{ CuZ (582 K)} > 6,0 \text{ CuZ (596 K)} > \text{HZSM-5 (640 K)} > 1,2 \text{ CuZ (669 K)}$$

#### 3.4. Temperature program surface reaction

Figures 5 and 6 show the TPSR profiles for the HZSM-5, 1,2 CuZ and 3,7 CuZ catalysts. These catalysts presented different behaviors, depending of the adopted experimental procedure in the TPSR analysis. When the sample was submitted first to the

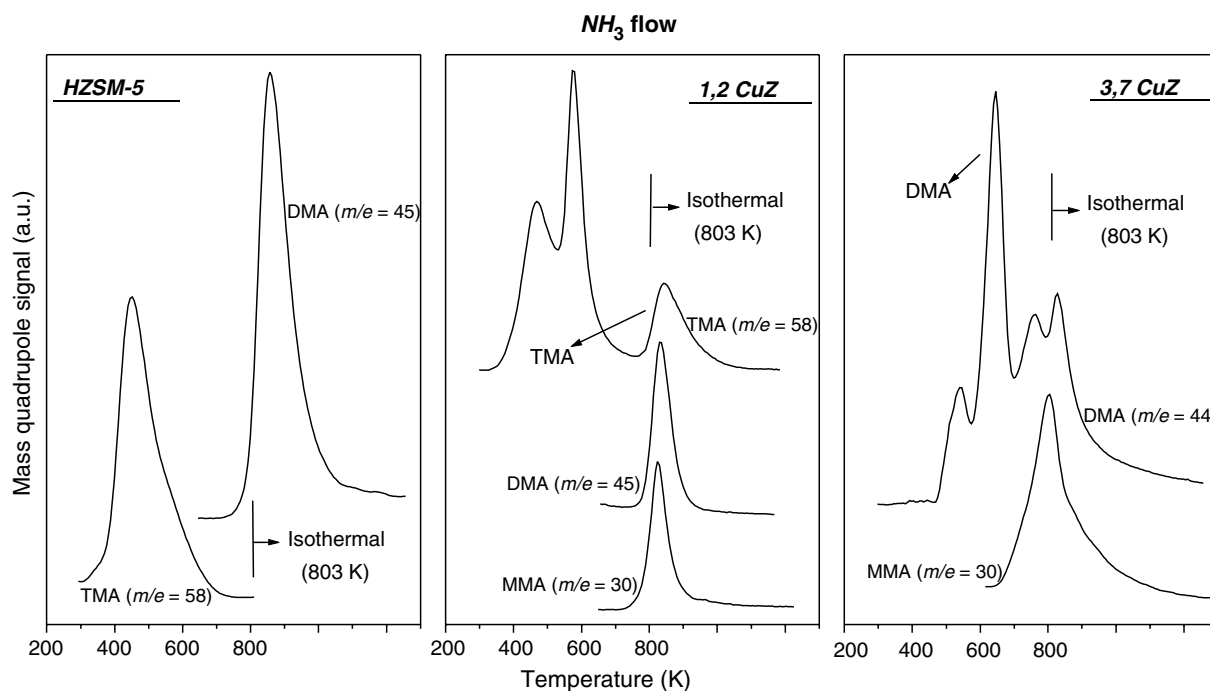


Figure 5. MMA, DMA and TMA profiles obtained during the TPSR analysis.

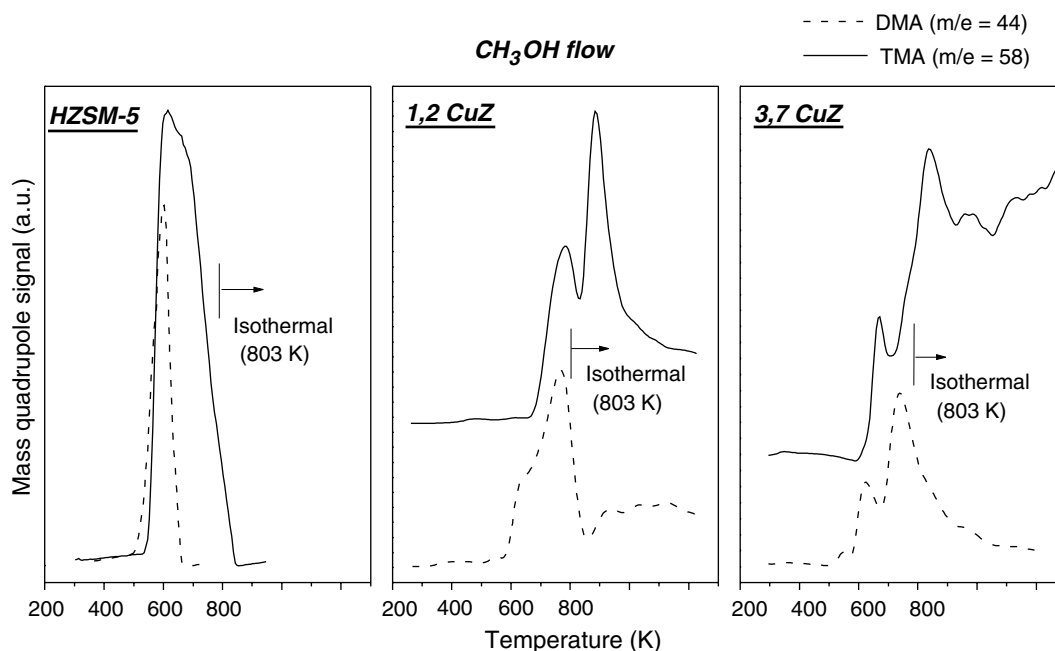


Figure 6. MMA, DMA and TMA profiles obtained during the TPSR analysis.

adsorption of methanol and subsequently to a flowing mixture  $\text{NH}_3/\text{He}$ , then amines desorption with increasing temperature changes with the catalyst. It shows that TMA was desorbed at lower temperature around 450 K on both cases, however, DMA and MMA desorbed at higher temperature around 803 K. However, on Cu catalysts this behavior changed. First, with increasing Cu content, DMA increases and the peaks are shifted to lower temperature, around 400–600 K, compared to the HZSM-5 or 1,2 CuZ catalysts.

The prior adsorption of methanol on the catalysts surface indicates that the amines formation can occur through either ammonia molecules present in gaseous phase and the methanol adsorbed on the catalyst surface. The prior adsorption of  $\text{NH}_3$  blocks the surface acid sites, hampers the methanol adsorption. In this case the reaction would occur between the adsorbed  $\text{NH}_3$  and the methanol present in the gaseous phase.

TMA is favored for higher Brönsted sites. These results suggest that the water released during the reduction of the CuO species present in the 3,7 and 6,0 CuZ catalysts modified the nature of acid sites, probably due to the dealumination of the zeolitic structure and, as consequence, the formation of extra-framework aluminium species. Then, the later would be the responsible by the increase in selectivity to MMA observed to the mentioned catalysts, in accordance with the literature [20,21].

During the  $\text{NH}_3$  adsorption and subsequent flow of a  $\text{CH}_3\text{OH}/\text{He}$  mixture, there is possible coke formation, which was also reported in previously for methanol on zeolites HZSM-5 [22–24].

Considering the acid character of these catalysts and the basic nature of the molecules involved in the reaction (ammonia and methylamines), it seems that these molecules would be strongly adsorbed on the acid sites, which explains the inaccessibility of methanol to the acid sites, as described above. When the temperature increases the adsorbed molecules are released and then the conversion increases. Concerning the zeolite HZSM-5 the effect of the temperature increase on the conversion was not sensible. It suggests that this behavior is related to the strong adsorption of molecules on the zeolites acid sites and depends on the nature of the acid sites, in particular the ratio of Brönsted/Lewis acid sites.

#### 4. Conclusion

The preparation of Cu/HZSM-5 catalysts showed that approximately 40% was ion exchanged and because of the pH variation after the ionic exchange step, there are CuO particle deposited at the external surface of the zeolite. However, the selectivity of MMA, DMA and TMA depends on the Cu content. Results showed that the activity increases with Cu and reaches a maximum rates for the 3.7% Cu content, which is also fairly more selective to MMA than the others metallic catalyst. The most important, is that the selectivity depends on the surface Lewis and Brönsted sites and not the total amount of acid sites. With increasing Cu content the Brönsted sites fall while the Lewis sites increases, and the best selectivity was obtained for a B/L ratio of approximately 1.

TPSR results with adsorbed methanol and  $\text{NH}_3$  flow confirms that the acid sites affect the selectivity and with the addition of Cu the maximum peak of DMA and MMA are shifted to lower temperatures. TMA is favored for higher Brönsted sites. It suggests that the water released during the reduction of the CuO catalysts change the nature of the acid sites, which in turn would be responsible for the increasing selectivity to MMA.

### Acknowledgments

CNPq for financial support and C. Souza, D. Dionizio and D. Vargas for technical support.

### References

- [1] D.L. King and J.H. Grate, *Chemtech*, April (1985) 244.
- [2] D.R. Corbin, S. Schwarz and G.C. Sonnichsen, *Catal. Today* 37 (1997) 71.
- [3] V.A. Veefkind and J.A. Lercher, *Appl. Catal. A: Gen.* 181 (1999) 245.
- [4] L.H. Callanan, E.V. Steen and C.T. O'Connor, *Catal. Today* 49 (1999) 229.
- [5] M. Pérez-Mendoza, M. Domingo-García and F.J. López-Garzón, *Appl. Catal. A: Gen.* 224 (2002) 239.
- [6] A. Baiker and J. Kijenski, *Catal. Rev. Sci. Eng.* 27 (1987) 653.
- [7] M. Iwamoto, H. Yahiro and S. Shundo, *Appl. Catal. A: Gen.* 69 (1991) L15.
- [8] D.V. Cesar, C.A.C. Perez, V.M.M. Salim and M. Schmal, *Appl. Catal. A: Gen.* 176 (1999) 205.
- [9] G.C. Bond and S.N. Namijo, *J. Catal.* 118 (1989) 507.
- [10] R. Bulánek, B. Wichterlová and Z. Sobalík, *Appl. Catal. B: Environ.* 131 (2001) 13.
- [11] M.C.N.A. de Carvalho, F.B. Passos, M. Schmal, *Appl. Catal.: Gen. A*, 193 (2000) 265.
- [12] T. Beutel, J. Sárkány and G.D. Lei, *J. Phys. Chem. B* 100 (1996) 845.
- [13] R.G. Herman e J.H. Lunsford, *J. Phys. Chem.* 79 (1975) 2388.
- [14] J. Sárkány, *Appl. Catal. A: Gen.* 188 (1999) 369.
- [15] A. Lucas, P. Canizares, A. Durán and A. Carrero, *Appl. Catal. A: Gen.* 154 (1997) 221.
- [16] S.M. Campbell, X.Z. Jiang and R.F. Howe, *Micropor. Mesopor. Mat.* 29 (1999) 91.
- [17] I. Mochida, A. Yasutake and H. Fujitsu, *J. Catal.* 82 (1983) 313.
- [18] E. Jobson, A. Baiker and A. Wokaun, *J. Chem. Soc. Faraday Trans.* 86(7) (1990) 1131.
- [19] A. Baiker and J. Kijenski, *Catal. Rev. Sci. Eng.* 27(4) (1985) 653.
- [20] C. Herrmann, F. Fetting and C. Plog, *Appl.Catal.* 39 (1988) 213.
- [21] Z. Hu, W. Lihui and S. Chen, *Micropor. and Mesopor. Mat.* 21 (1998) 7.
- [22] F.J. Keil, *Micropor. Mesopor. Mat.* 29 (1999) 49.
- [23] K.P. Möller, W. Böhringer and A.E. Schnitzler, *Micropor. Mesopor. Mat.* 29 (1999) 127.
- [24] S.M. Campbell, X.Z. Jiang and R.F. Howe, *Micropor. Mesopor. Mat.* 29 (1999) 91.